Highly Tunable Charge Transport in Layer-by-Layer Assembled Graphene Transistors

Hyunmin Hwang,[†,#] Piljae Joo,[‡,#] Moon Sung Kang,[§] Gukmoon Ahn,[‡] Joong Tark Han,[⊥] Byeong-Su Kim,[‡,*] and Jeong Ho Cho[∥,*]

[†]Department of Organic Materials and Fiber Engineering, Soongsil University, Seoul 156-743, Korea, [‡]Interdisciplinary School of Green Energy, KIER-UNIST Advanced Center for Energy and Low Dimensional Carbon Materials Center, Ulsan National Institute of Science and Technology (UNIST), Ulsan 689-798, Korea, [§]Department of Chemical Engineering, Soongsil University, Seoul 156-743, Korea, [⊥]Nano Carbon Materials Research Group, Korea Electrotechnology Research Institute, Changwon 641-120, Korea, and [∥]SKKU Advanced Institute of Nanotechnology (SAINT) and Center for Human Interface Nano Technology (HINT), Department of Chemical Engineering, Sungkyunkwan University, Suwon 440-746, Korea. [#] These authors contributed equally to this work.

ABSTRACT We demonstrate a controlled, systematic method to tune the charge transport in graphene field-effect transistors based on alternating layer-by-layer assembly of positively and negatively charged graphene oxide followed by thermal reduction. Surprisingly, tuning the number of bilayers of thermally reduced graphene oxide multilayer films allowed achieving either ambipolar or unipolar (both n- and p-type) transport in graphene transistors. On the basis of X-ray photoemission spectroscopy, Raman spectroscopy, time-of-flight secondary ion mass spectrometry, and temperature-dependent charge transport measurements, we found that nitrogen atoms from the functional groups of positively charged graphene oxide are incorporated into the reduced graphene oxide films and substitute carbon atoms during the thermal reduction. This nitrogen-doping process occurs in different degrees for graphene multilayers with varying numbers of bilayers and thereby results in the interesting transition in the electrical behavior in graphene multilayer transistors. We believe that such a versatile method to control the charge transport in graphene multilayers will further promote their applications in solution-processable electronic devices based on graphene.

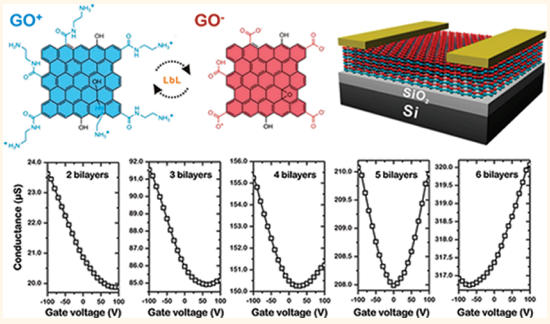

KEYWORDS: graphene · layer-by-layer assembly · nitrogen doping · ambipolar to unipolar transition · transistor

Since its first discovery, graphene, a monolayer of a two-dimensional carbon lattice, has emerged as a promising nanomaterial in various fields.[1−6] In particular, its superior electronic properties exhibiting ballistic transport at room temperature and high intrinsic carrier mobility, excellent chemical and mechanical stability, and outstanding thermal conductivity make graphene an ideal candidate for future electronic device and sensor applications.[7−12] As a consequence, early efforts were focused on incorporating graphene into a field-effect transistor (FET), and recently complicated logic gates based on ambipolar graphene FETs have been demonstrated toward achieving high-speed integrated electronic circuits.[13,14] Furthermore, from a practical point of view, methods have been developed to deposit graphene onto various substrates by a solution process, which provides versatile opportunities to employ graphene in low-cost, flexible electronic applications.

To further exploit the superior characteristics of graphene in electronic applications, achieving unipolar transport in graphene (n- and p-type transport separately) is critical. This is because employing both n- and p-type unipolar transport devices in a complementary manner is highly desirable for low power consumption in complex logic circuits compared to those based on ambipolar transport. Accordingly, various recent efforts have been developed to access unipolar conduction in graphene, including tuning the band gap *via* downsizing to nanoribbons,[15−18] introducing impurities or chemical doping,[19] controlling the interface polarization *via* a self-assembled monolayer,[20,21] and controlling the charge-density pinning effect at metal contacts.[22,23] Although a moderate shift in the Dirac voltage and a slight enhancement/suppression in the respective carrier mobility were observed, many of these approaches still yielded an ambipolar transport behavior in graphene. It is only recent that Li and co-workers reported a complementary logic inverter based on true n- and p-type unipolar graphene transistors by controlling the doping density in graphene using titanium oxide.[24]

Alternatively, we present herein a simple approach to control the charge transport in

* Address correspondence to jhcho94@skku.edu; bskim19@unist.ac.kr.

Received for review December 4, 2011 and accepted February 7, 2012.

Published online February 07, 2012
10.1021/nn2047197

graphene based on a layer-by-layer (LbL) assembly between positively and negatively charged graphene oxide (GO) and a subsequent thermal reduction process.[25,26] As a true nanoscale blending method, the LbL assembly offers a unique opportunity to prepare multilayer thin films of graphene of desired composition with a precise nanometer scale control over the thickness (*e.g.*, the number of graphene sheets). Surprisingly, the fine control over the number of bilayers resulted in a dramatic transition in the charge transport from p-type unipolar, to ambipolar, and eventually to n-type unipolar transport with the increase in the number of graphene bilayers from two to six. Unlike thermally reduced graphene oxide (TRGO) multilayer films, chemically reduced graphene oxide (CRGO) multilayer films exhibited only an ambipolar transport behavior regardless of the number of bilayers. On the basis of X-ray photoemission spectroscopy, Raman spectroscopy, and time-of-flight secondary ion mass spectrometry analysis, we find that such an interesting transition in the charge transport behavior of multilayer TRGO films is due to more nitrogen atoms (from the surface functional groups of positively charged GO) being incorporated into thicker GO multilayers, which results in n-type doping of the graphene films upon thermal reduction. In addition, a temperature-dependent charge transport study was carried out to further examine the influence of the number of bilayers on the conduction in graphene multilayer systems for the first time. The results also revealed the increased nitrogen doping in the TRGO films with increasing number of bilayers. We believe that this method offers a versatile opportunity to achieve unipolar (either n- or p-type) and ambipolar graphene FETs in a controlled manner.

RESULTS AND DISCUSSION

The multilayer graphene films were prepared by sequential LbL assembly between positively and negatively charged GO sheets and subsequent thermal (or chemical) reduction. Negatively charged graphene oxide suspensions (GO^-) were prepared according to the modified Hummers method with pure graphite followed by exfoliation under ultrasonication.[27,28] Separately, positively charged stable GO suspensions (GO^+) were prepared by introducing amine groups (NH_2) on the surface of negatively charged GO sheets through the *N*-ethyl-*N*′-(3-dimethylaminopropyl)carbodiimide methiodide (EDC)-mediated reaction between carboxylic acids (and/or epoxides) and excess ethylenediamine ($NH_2CH_2CH_2NH_2$) (Figure S1 in the Supporting Information). As-prepared respective GO suspensions exhibited a fairly good colloidal stability over a wide span of pH conditions. They also displayed changes in zeta-potential in response to external pH conditions, which is a typical pH-responsive feature of weak polyelectrolytes.[25,29] With these two stable suspensions of GO^+ and GO^-, we have fabricated GO multilayer films by repeatedly spin-coating onto a planar SiO_2/Si substrate or a quartz slide to afford the multilayer in a $(GO^+/GO^-)_n$ architecture (n = number of bilayers, typically n = 2–6) (Figure 1). Finally, the GO multilayers were subjected to either a thermal reduction process (1000 °C under Ar) or a chemical hydrazine reduction to afford multilayers of RGO following well-documented protocols.[25,30–34]

The successful growth of GO multilayers was monitored *via* a gradual increase of the UV/vis absorbance spectra with a characteristic absorbance of GO within the multilayer film of 222 nm (Figure 2a). This peak red-shifts to 275 and 268 nm after thermal and chemical reduction, respectively, which indicates the successful restoration of electronic conjugation within the graphene sheets (Figure 2b and Figure S2 in the Supporting Information). The UV/vis absorbance spectra of the corresponding TRGO and CRGO films also exhibited a gradual increase with increasing number of bilayers.

Consistent with the UV/vis absorption spectra, the ellipsometry measurement showed that the thickness of GO multilayer films is linearly proportional to the number of bilayers, demonstrating true LbL assembly of GO multilayers (Figure 2c). Note that the thickness of GO films decreased upon chemical or thermal reduction due to the loss of surface functional groups, as similarly observed in our previous report.[25] From the linear fitting of the curves, the average bilayer thickness of GO, TRGO, and CRGO is calculated to be 1.6, 0.6, and 1.1 nm, respectively.

Figure 2c shows the atomic force microscopy (AFM) images of two- and six-bilayered GO and TRGO films. Initial few-layer depositions (less than two bilayers) displayed overlaid sheets of GO, though the complete substrate was not covered as often observed in the initial few layers of polyelectrolyte-based LbL systems. As the deposition progresses to more than three bilayers, however, the entire surface was uniformly covered with GO (Figure S3 in the Supporting Information). Interestingly, the edges of individual graphene sheets are clearly visible in an as-assembled GO multilayer film, whereas the individual sheets appear to merge together and leave no distinct boundary between each sheet after thermal annealing. In addition, surface root-mean-square roughness (R_{rms}) values (averaged over 10 × 10 μm^2) of two and six bilayers were determined to be 1.4 and 2.5 nm, respectively. After thermal reduction, these values decreased to 0.4 and 0.8 nm, respectively. The decreased surface roughness is ascribed to the reorientation of GO sheets and densification of the thin film during thermal annealing.

The electrical characteristics of the as-prepared LbL-assembled graphene films were investigated by employing graphene FETs. Specifically, the graphene FETs were fabricated by assembling multilayer graphene films on a heavily doped Si wafer with a thermally grown 300 nm thick SiO_2 layer. The Si wafer itself and

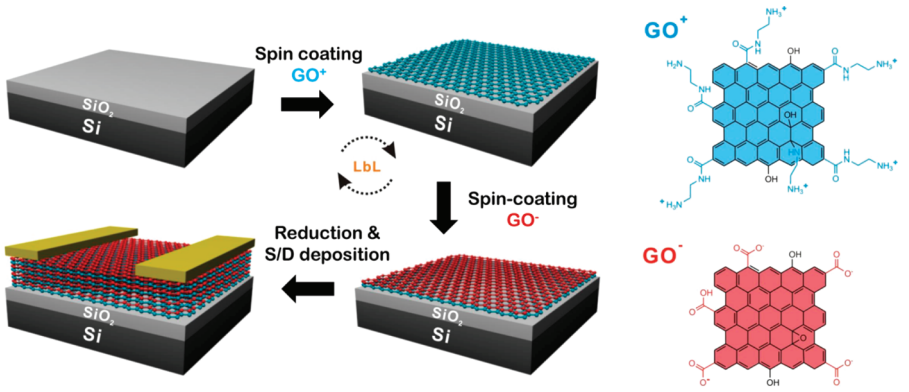

Figure 1. Schematic representation of LbL-assembled graphene-based FETs.

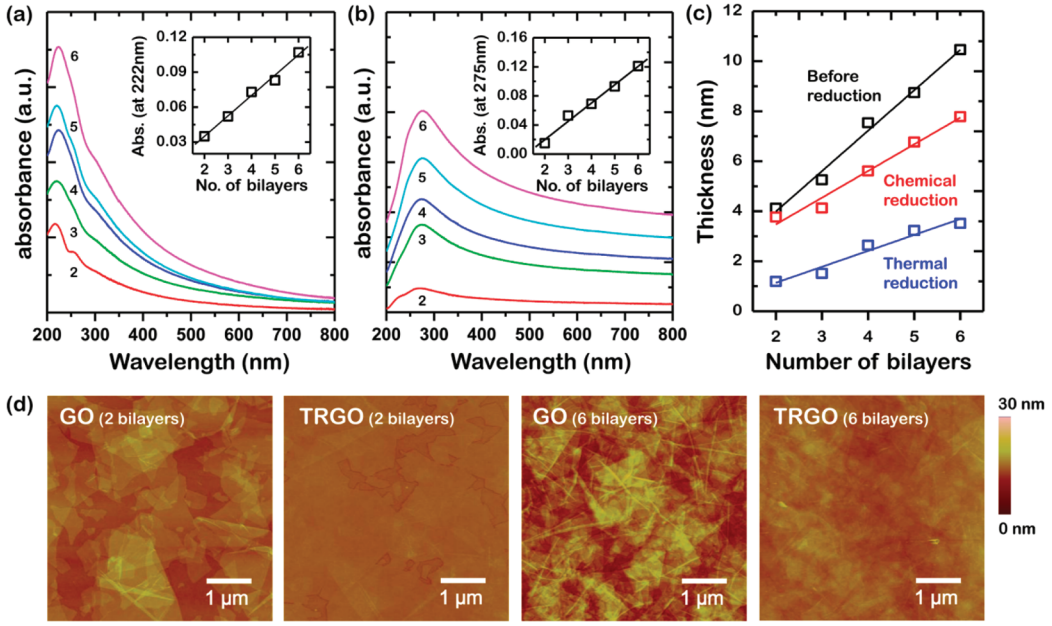

Figure 2. UV/vis absorbance spectra of (a) GO and (b) TRGO with different numbers of graphene bilayers. Insets show the linear relation between the absorbance at the peak and the number of bilayers. (c) Film thickness *vs* number of graphene bilayers. (d) AFM images of two- and six-bilayered GO and TRGO.

the SiO_2 layer worked as the gate electrode and the gate dielectric, respectively. Au contacts that were deposited on top of the graphene film by thermal evaporation served as the source and drain electrodes (Figure 1). The channel length (L) and channel width (W) were 100 and 800 μm, respectively.

Figure 3a shows the conductance (G) *vs* V_G plots of TRGO FETs with different numbers of graphene bilayers. Surprisingly, we observed that the charge transport in TRGO FETs changes dramatically, along with an expected increase in the film conductance (Figure 3b) upon varying the number of bilayers. TRGO FETs with two bilayers exhibited unipolar p-type conduction, unlike typical graphene FETs, which generally yield ambipolar transport.[35] A similar result was observed previously from a mechanically cleaved monolayer graphene, which was explained by a positive charge transfer from the SiO_2 substrate during thermal treatment.[12] As the number of bilayers increased, the influence of the SiO_2 substrate was reduced concomitantly, while n-type conduction appeared gradually and the Dirac voltage shifted accordingly to more negative voltage (Figure 3c). As a consequence, a symmetric ambipolar transport was observed from five-bilayered TRGO films and even unipolar n-type conduction was observed from six-bilayered TRGO films. These results indicated that more electron doping is taking place as the number of bilayers increases. Note that such a dramatic change in the charge transport from nearly p-type to ambipolar and even to n-type transport and a Dirac voltage shift of 133 V (from 78 V to −55 V) occurred only within a difference of four bilayers of TRGO films. We carried out a similar experiment based on LbL-assembled CRGO FETs (Figure S4 in the Supporting Information). However, no significant change in the transport type or a shift in the Dirac voltage was observed upon varying the film

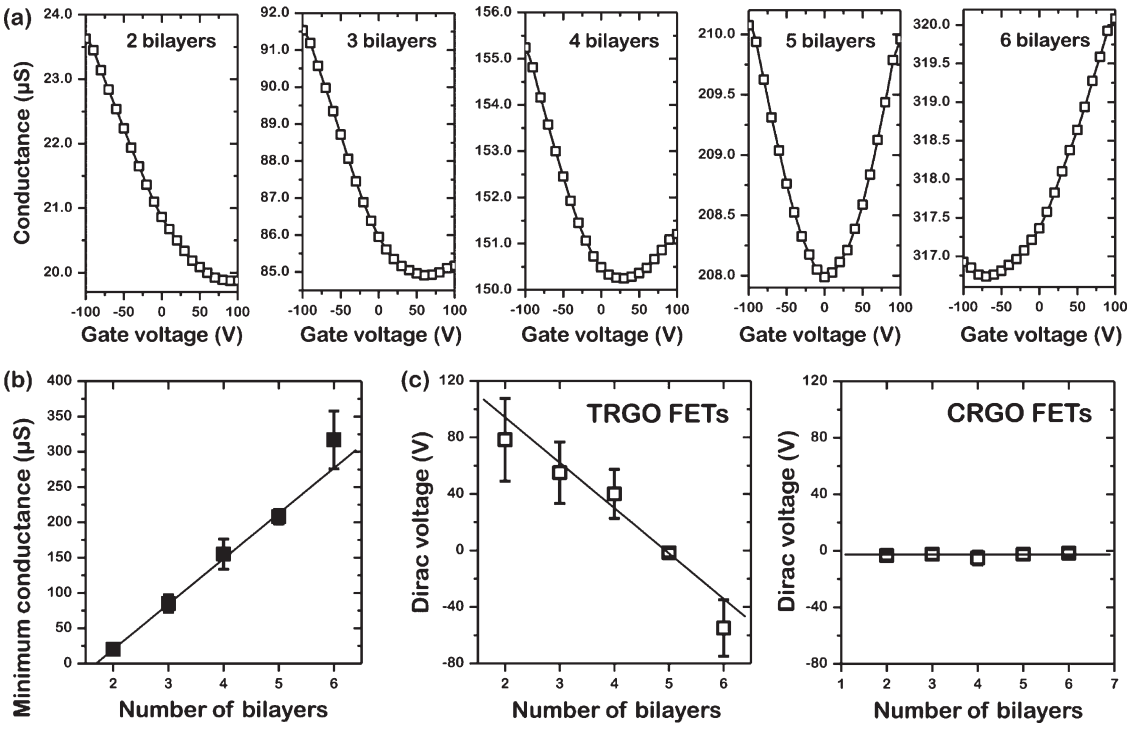

Figure 3. (a) Transfer characteristics of TRGO FETs with various numbers of graphene bilayers. (b) Minimum conductance of TRGO FETs as a function of the number of graphene bilayers. (c) Dirac voltage changes in TRGO- and CRGO-based FETs as a function of number of graphene bilayers.

thickness (Figure 3c). These results suggest that n-type doping did not occur during the chemical reduction and that the thermal annealing during the reduction process plays an important role in electron doping of multilayer graphene films.

To study the influence of thermal annealing and the origin of consequent electron doping, we have employed several independent techniques. First, X-ray photoemission spectroscopy (XPS) was performed to investigate the changes of chemical functional groups during the thermal (and chemical) reduction process. Figure 4a shows the high-resolution XPS spectra of the two-bilayer TRGO, CRGO, and GO films. The deconvoluted C1s spectra of the GO film exhibited five distinct components, including sp^2-hybridized carbons (284.5 eV), C−O in epoxy and hydroxyl (286.2 eV), carbonyls (286.8 eV), amides (287.9 eV), and carboxylic acids (288.9 eV), which are all in good agreement with previous reports.[36−38] The intensities of the peaks assigned to the oxygen-bearing functional groups such as hydroxy, epoxy, and carbonyl groups almost disappeared after thermal reduction, as expected. Interestingly, a new peak located at 285.9 eV appeared, corresponding to C−N with sp^2-hybridized carbon,[37] although the thermal reduction was performed in nitrogen-free conditions. In contrast, after chemical reduction, the peak associated with the C−N with an sp^2-hybridized carbon was not observed, although peaks from oxygen moieties were removed considerably. These results indicate that the nitrogen atoms in amide and amine groups within the positively charged GO are incorporated into the graphene layer and substitute carbon atoms only during the thermal annealing process. Furthermore, we found that the relative amount of carbon atoms yielding a C_{sp2}-N (285.9 eV) signal increases with increasing number of bilayers (Figure 4b and c). This result suggests that more nitrogen atoms are introduced into the graphene as the film thickness increases and supports results from the electrical transport measurements (more n-type transport for thicker films).

In accord with the above results, N1s spectra yielded more detailed information about the change in the chemical states of graphene films after thermal (and chemical) reduction. The N1s peak in the two-bilayer GO film has two components, centered at 399.6 and 402.5 eV, corresponding to amides and amines, respectively, which arise from the chemically modified positively charged GO (Figure 4a). Interestingly, new types of nitrogen species appeared after thermal reduction at 398.6, 400.3, and 401.1 eV, which can be assigned to pyridinic-N, pyrrolic-N, and graphitic-N, respectively.[37,38] In contrast, these new peaks were not observed after chemical reduction with hydrazine, although the signals corresponding to amines were dramatically reduced. These new peaks support that the N atoms are substitutionally doped into the graphene lattice after thermal reduction at high temperature. Also, the relative amount of graphitic-N (401.1 eV) increased with the number of bilayers in TRGO films, reflecting more substitutional

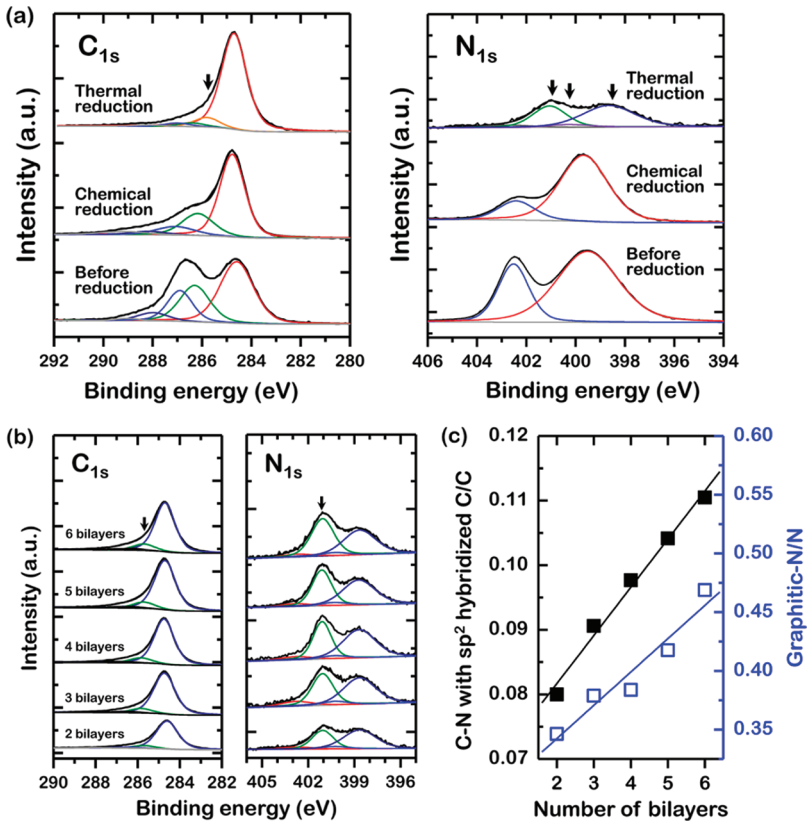

Figure 4. (a) High-resolution XPS C1s and N1s spectra of two-bilayer TRGO, CRGO, and GO films. Arrows indicate C_{sp2}-N in C1s and graphitic-N, pyrrolic-N, and pyridinic-N in N1s, respectively, after thermal reduction. (b) High-resolution XPS C1s and N1s spectra of TRGO films with various numbers of graphene bilayers. (c) Atomic ratio of C_{sp2}-N C and graphitic-N obtained from XPS C1s and N1s spectra of TRGO films.

nitrogen doping into the graphitic layer for thicker films (Figure 4b and c). From the XPS measurement, we estimated approximately 1.64% nitrogen is doped into the six-bilayer TRGO film. The explanation for this trend, which was also observed from the C1s XPS data and the electrical transport measurements, is as follows. Nitrogen species such as amines and amides would be removed from the surfaces of graphene sheets, probably in the form of N_2 gas during the thermal annealing process, as observed in another report.[30] However, the stacked and confined geometry of the LbL-assembled multilayer films possibly prevents facile escape of the nitrogen species. Therefore, more fractions of nitrogen species are likely to reside within the film with more graphene layers, thereby resulting in a higher nitrogen-doping concentration per unit volume of carbon lattice. Although the detailed mechanism of nitrogen doping onto the multilayer graphene film is still elusive, note that a similar approach was employed in the synthesis of nitrogen-doped graphenes by mixing chemically modified graphene oxide with nitrogen-rich compounds such as melamine under a high-temperature annealing process.[38] It should be noted that the number of bilayers is the key factor in modulating both the nitrogen-doping level and electrical conductance of graphene films. These interesting features highlight the advantages of LbL assembly as a nanoscale bottom-up assembly technique that is otherwise hard to achieve with other methods.

Raman spectroscopy is the most direct and nondestructive technique to characterize the structure of carbon materials. The evolution of the Raman spectra is presented in Figure 5a as a function of the number of graphene bilayers in TRGO films. The Raman spectra were obtained with excitation at 532 nm for 10 s to avoid overheating of the samples. A significant red-shift (ca. 19 cm^{-1}) of the G band was observed as the number of graphene bilayers increased, while the D band remained fixed. This red-shift of the G band implies an electron-doping effect in the TRGO films, as it is suggested that electron doping upshifts the Fermi level away from the Dirac point.[39−42] In contrast, CRGO films did not exhibit any shift in the G band upon varying the number of bilayers (Figure S5 in the Supporting Information).

In addition, a time-of-flight secondary ion mass spectrometry (TOF-SIMS) analysis was carried out, which also supported that the relative amount of nitrogen atoms increased with the number of bilayers in TRGO films (Figure 5c and Figure S6 in the Supporting Information). For example, the negative ion spectrum demonstrated the presence of CN^- (m/z = 26) and N^- (m/z = 14), which increased with the number of TRGO

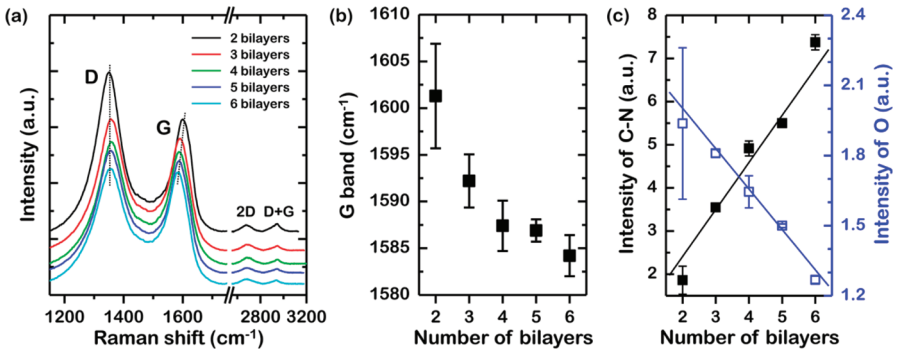

Figure 5. (a) Raman spectra of TRGO films with various numbers of graphene bilayers. (b) Raman G bands as a function of the number of graphene bilayers. (c) Intensities of C-N and O as a function of the number of graphene bilayers obtained from TOF-SIMS measurements.

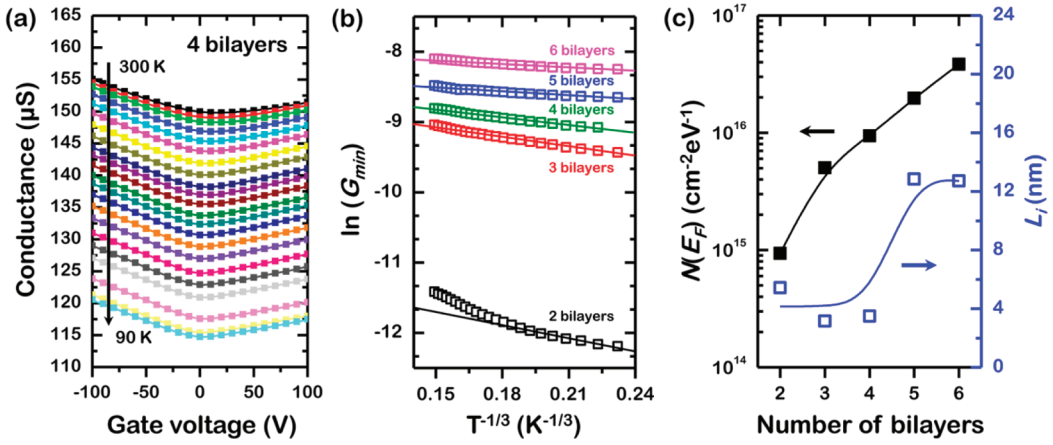

Figure 6. (a) Temperature-dependent conductance *vs* gate voltage plots of TRGO FETs with four-bilayer TRGO FET. (b) $\ln(G_{min})$ *vs* $T^{-1/3}$ plots of TRGO FETs with different numbers of graphene bilayers. (c) $N(E_F)$ and L_i of TRGO films as a function of number of bilayers.

bilayers, confirming the development of nitrogen doping in multilayer TRGO films. We also observed that the intensity of O^- ($m/z = 16$) decreased upon progress of nitrogen doping, which would possibly displace the defect sites that are occupied by oxygen on the graphene sheets.

Finally, the charge transport mechanism in LbL-assembled TRGO multilayer films was investigated as a function of bilayer numbers through temperature-dependent transport measurements.[43−45] It should be mentioned here that the integration of graphenes and related nanostructures into multilayer films by LbL assembly has been recently demonstrated from a number of examples;[25,26,30,46−51] however, many of these studies are limited to the enhancement of electrical conductivity without addressing systematic efforts in elucidating the key components in the charge transport mechanism as a function of bilayer numbers. To the best of our knowledge, this is the first attempt to associate the temperature-dependent charge transport study with the number of graphene layers.

Figure 6a shows representative transfer characteristics of TRGO FETs with four graphene bilayers, for example, over the range between 300 and 90 K. With decreasing temperature, the conductance decreased, while the on/off current ratio increased slightly. The Dirac voltage approached 0 V, and the *V*-shape of the ambipolar characteristics became more pronounced at lower temperatures. A similar trend has been observed from an individual monolayer of RGO.[52] For more careful investigation, we examined the temperature dependence of the minimum conductance (G_{min}) of RGO instead of G at $V_G = 0$ V, to exclude the effect of charged impurities. A plot of $\ln(G_{min})$ as a function of $T^{-1/3}$ showed a reasonable linear fit, suggesting that the 2D-variable range hopping (VRH) model describes the charge transport in graphene multilayer films (Figure 6b).[35] In this model, the temperature-dependent conductance of the 2D-VRH model can be described as

$$G = A \exp\left(-\frac{B}{T^{1/3}}\right) \quad (1)$$

The parameter A is given by

$$A = \frac{eR_o{}^2 \nu_{ph}}{k_B}$$

where k_B is the Boltzmann constant, R_o is the optimum hopping distance, and ν_{ph} is the frequency of the

phonons associated with the hopping process. The hopping parameter B is given by

$$B = \left(\frac{3}{k_B N(E_F) L_l^2}\right)^{1/3}$$

where $N(E_F)$ and L_l are the density of states near the Fermi level and the localization length of the electronic wave function, respectively. One can estimate B values for TRGO films based on different numbers of graphene bilayers from the slope of the $\ln(G_{min})$ *vs* $T^{-1/3}$ plot. Furthermore, $N(E_F)$ and L_l for these TRGO films can be estimated by the method described previously.[53] As summarized in Figure 6c, it was estimated that the density of states at E_F increases dramatically from 9.36×10^{14} to 9.84×10^{16} cm^{-2} as the number of bilayers increases from 2 to 6. This result is consistent with the results based on other characterizations such as XPS, Raman spectra, and TOF-SIMS analysis, which suggests that more nitrogen doping takes place in TRGO films with increased bilayer thickness. Also, we estimated that L_l increases from 5.4 to 12.7 nm with an increasing number of bilayers. This is because the increased electron concentration by n-type doping can fill the traps in the defect sites of a graphene lattice and thereby elongate the electronic wave function.

CONCLUSIONS

In summary, we demonstrated a simple method to achieve unipolar transport in graphene FETs by employing LbL assembly of positively and negatively charged graphene oxide nanosheets, followed by thermal reduction. Surprisingly, the charge transport in thermally reduced GO multilayer films could be tuned from p-type to ambipolar to n-type by precisely controlling the number of bilayers of graphene, unlike a typical ambipolar transport observed from chemically reduced GO multilayer films. From various characterization techniques, we concluded that this unique tunable charge transport in LbL-assembled graphene is a result of different degrees of nitrogen doping to graphene multilayers with different thickness during the thermal annealing process. Considering the versatile nature of LbL assembly coupled with the extraordinary electronic properties of the graphene, we envision this study will offer opportunities and insights for further development of solution-processable graphene-based electronic devices.

METHODS

Preparation of Negatively and Positively Charged GO. Graphite oxide was synthesized by the modified Hummers method[27,28] and exfoliated under ultrasonication to yield a brown dispersion of graphene oxide in water. The resulting graphene oxide is negatively charged over a wide span of pH conditions due to the presence of chemical functional groups such as carboxylic acids. Positively charged GO was synthesized by mixing 1.25 g of EDC (Sigma Aldrich) and 10 mL of ethylenediamine (99%, Sigma Aldrich) into 100 mL of GO^- suspension (0.5 mg/mL) and left stirring for 12 h. The resulting suspension was dialyzed (MWCO 12 000−14 000, Spectra/Por) for 3 days to remove any residues and byproduct. Prior to LbL deposition, the pH of the GO^+ and GO^- suspension was adjusted to 3.5 and 10, respectively.

Layer-by-Layer Assembly. Silicon or quartz substrates were cleaned by piranha solution to remove any organic contamination and treated with oxygen plasma to introduce a hydrophilic surface. The positively charged GO suspension (0.5 mg/mL) at pH 3.5 was first dispensed onto a silicon or a quartz substrate and allowed to self-assemble for 2 min prior to spin-coating at 3000 rpm for 30 s (ACE-200, Dong Ah Tech). Then, pH-adjusted deionized water was dropped on the positively charged GO film, as a rinsing step. Next, a negatively charged GO solution (0.5 mg/mL) at pH 10 was spin-coated onto the as-assembled positively charged GO film, following an identical procedure to afford a one-bilayer film of a $(GO^+/GO^-)_1$ multilayer. The above procedures were repeated to achieve the desired number of graphene bilayers. These as-assembled GO multilayer films were subjected to thermal or chemical reduction. The thermal reduction of the GO multilayer film was carried out by heating the sample in a furnace under an argon atmosphere. The temperature was raised to 1000 °C at a rate of 15 °C/min and maintained at that temperature for 30 min before cooling it to room temperature. The chemical reduction of the GO multilayer film typically involved a hydrazine vapor treatment at 80 °C. After 24 h of hydrazine reduction, the CRGO films were isolated and dried at room temperature.

Characterization. The absorbance of the films was characterized by using UV/vis spectroscopy (Varian, Cary 5000), and the thickness of the GO multilayer films on a silicon wafer was characterized with ellipsometry (EC-400 and M-2000 V, J. A. Woollam Co. Inc.). Surface morphology of the samples was investigated by a tapping mode AFM (D3100 Nanoscope V, Veeco). The transistor current−voltage characteristics were measured using Keithley 2400 and 236 source/measure units under vacuum (10^{-5} Torr). The temperature-dependent transport measurements were conducted in a cryostat (ST-500, Janis) with a base pressure of 10^{-5} Torr over the range 90−300 K. The functional groups of GO multilayer films were analyzed with XPS (K-alpha, Thermo Fisher) and TOF-SIMS (TOF SIMS5, ION TOF). The structural characterization of the GO multilayer films was carried out using a confocal Raman spectrometer (NT-MDT, NTEGRA SPECTRA) with a 532 nm excitation wavelength.

Conflict of Interest: The authors declare no competing financial interest.

Acknowledgment. This work is dedicated in memory of our old friend Dr. Sungho Choi. This research is supported by WCU (World Class University) Program through the Korea Science and Engineering Foundation funded by the Ministry of Education, Science and Technology (R31-2008-000-20012-0), the National Research Foundation of Korea (NRF) grants (2010-0003219 and 2009-0083540), and a grant (Code No. 2011-0031639) from the Center for Advanced Soft Electronics under the Global Frontier Research Program of the Ministry of Education, Science and Technology, Republic of Korea.

Supporting Information Available: Additional characterization data of UV/vis, AFM, TOF-SIMS, Raman, and transistor measurements. This material is available free of charge *via* the Internet at http://pubs.acs.org.

REFERENCES AND NOTES

1. Geim, A. K.; Novoselov, K. S. The Rise of Graphene. *Nat. Mater.* **2007**, *6*, 183–191.

2. Wu, J. S.; Pisula, W.; Mullen, K. Graphenes as Potential Material for Electronics. *Chem. Rev.* **2007**, *107*, 718–747.
3. Kim, K. S.; Zhao, Y.; Jang, H.; Lee, S. Y.; Kim, J. M.; Ahn, J. H.; Kim, P.; Choi, J. Y.; Hong, B. H. Large-Scale Pattern Growth of Graphene Films for Stretchable Transparent Electrodes. *Nature* **2009**, *457*, 706–710.
4. Balandin, A. A.; Ghosh, S.; Bao, W. Z.; Calizo, I.; Teweldebrhan, D.; Miao, F.; Lau, C. N. Superior Thermal Conductivity of Single-Layer Graphene. *Nano Lett.* **2008**, *8*, 902–907.
5. Stankovich, S.; Dikin, D. A.; Dommett, G. H. B.; Kohlhaas, K. M.; Zimney, E. J.; Stach, E. A.; Piner, R. D.; Nguyen, S. T.; Ruoff, R. S. Graphene-Based Composite Materials. *Nature* **2006**, *442*, 282–286.
6. Geim, A. K. Graphene: Status and Prospects. *Science* **2009**, *324*, 1530–1534.
7. Castro Neto, A. H.; Guinea, F.; Peres, N. M. R.; Novoselov, K. S.; Geim, A. K. The Electronic Properties of Graphene. *Rev. Mod. Phys.* **2009**, *81*, 109–162.
8. Morozov, S. V.; Novoselov, K. S.; Katsnelson, M. I.; Schedin, F.; Elias, D. C.; Jaszczak, J. A.; Geim, A. K. Giant Intrinsic Carrier Mobilities in Graphene and its Bilayer. *Phys. Rev. Lett.* **2008**, *100*, 016602.
9. Novoselov, K. S.; Geim, A. K.; Morozov, S. V.; Jiang, D.; Katsnelson, M. I.; Grigorieva, I. V.; Dubonos, S. V.; Firsov, A. A. Two-Dimensional Gas of Massless Dirac Fermions in Graphene. *Nature* **2005**, *438*, 197–200.
10. Novoselov, K. S.; Jiang, Z.; Zhang, Y.; Morozov, S. V.; Stormer, H. L.; Zeitler, U.; Maan, J. C.; Boebinger, G. S.; Kim, P.; Geim, A. K. Room-Temperature Quantum Hall Effect in Graphene. *Science* **2007**, *315*, 1379–1379.
11. Zhang, Y. B.; Tan, Y. W.; Stormer, H. L.; Kim, P. Experimental Observation of the Quantum Hall Effect and Berry's Phase in Graphene. *Nature* **2005**, *438*, 201–204.
12. Wang, S.; Ang, P. K.; Wang, Z. Q.; Tang, A. L. L.; Thong, J. T. L.; Loh, K. P. High Mobility, Printable, and Solution-Processed Graphene Electronics. *Nano Lett.* **2010**, *10*, 92–98.
13. Palacios, T.; Hsu, A.; Wang, H. Applications of Graphene Devices in RF Communications. *IEEE Commun. Mag.* **2010**, *48*, 122–128.
14. Wang, H.; Nezich, D.; Kong, J.; Palacios, T. Graphene Frequency Multipliers. *IEEE Electron Device Lett.* **2009**, *30*, 547–549.
15. Li, X. L.; Wang, X. R.; Zhang, L.; Lee, S. W.; Dai, H. J. Chemically Derived, Ultrasmooth Graphene Nanoribbon Semiconductors. *Science* **2008**, *319*, 1229–1232.
16. Zhu, Y.; Tour, J. M. Graphene Nanoribbon Thin Films Using Layer-by-Layer Assembly. *Nano Lett.* **2010**, *10*, 4356–4362.
17. Chen, Z. H.; Lin, Y. M.; Rooks, M. J.; Avouris, P. Graphene Nano-Ribbon Electronics. *Phys. E* **2007**, *40*, 228–232.
18. Han, M. Y.; Özyilmaz, B.; Zhang, Y.; Kim, P. Energy Band-Gap Engineering of Graphene Nanoribbons. *Phys. Rev. Lett.* **2007**, *98*, 206805.
19. Li, X. L.; Wang, H. L.; Robinson, J. T.; Sanchez, H.; Diankov, G.; Dai, H. J. Simultaneous Nitrogen Doping and Reduction of Graphene Oxide. *J. Am. Chem. Soc.* **2009**, *131*, 15939–15944.
20. Lee, B.; Chen, Y.; Duerr, F.; Mastrogiovanni, D.; Garfunkel, E.; Andrei, E. Y.; Podzorov, V. Modification of Electronic Properties of Graphene with Self-Assembled Monolayers. *Nano Lett.* **2010**, *10*, 2427–2432.
21. Lee, W. H.; Park, J.; Kim, Y.; Kim, K. S.; Hong, B. H.; Cho, K. Control of Graphene Field-Effect Transistors by Interfacial Hydrophobic Self-Assembled Monolayers. *Adv. Mater.* **2011**, *23*, 3460–3464.
22. Nouchi, R.; Shiraishi, M.; Suzuki, Y. Transfer Characteristics in Graphene Field-Effect Transistors with Co Contacts. *Appl. Phys. Lett.* **2008**, *93*, 152104.
23. Nouchi, R.; Tanigaki, K. Charge-Density Depinning at Metal Contacts of Graphene Field-Effect Transistors. *Appl. Phys. Lett.* **2010**, *96*, 253503.
24. Li, H.; Zhang, Q.; Liu, C.; Xu, S. H.; Gao, P. Q. Ambipolar to Unipolar Conversion in Graphene Field-Effect Transistors. *ACS Nano* **2011**, *5*, 3198–3203.
25. Lee, D. W.; Hong, T. K.; Kang, D.; Lee, J.; Heo, M.; Kim, J. Y.; Kim, B. S.; Shin, H. S. Highly Controllable Transparent and Conducting Thin Films Using Layer-by-Layer Assembly of Oppositely Charged Reduced Graphene Oxides. *J. Mater. Chem.* **2011**, *21*, 3438–3442.
26. Hong, J.; Han, J. Y.; Yoon, H.; Joo, P.; Lee, T.; Seo, E.; Char, K.; Kim, B. S. Carbon-Based Layer-by-Layer Nanostructures: from Films to Hollow Capsules. *Nanoscale* **2011**, 4515–4531.
27. Hummers, W. S.; Offeman, R. E. Preparation of Graphitic Oxide. *J. Am. Chem. Soc.* **1958**, *80*, 1339–1339.
28. Kovtyukhova, N. I.; Ollivier, P. J.; Martin, B. R.; Mallouk, T. E.; Chizhik, S. A.; Buzaneva, E. V.; Gorchinskiy, A. D. Layer-by-Layer Assembly of Ultrathin Composite Films from Micron-Sized Graphite Oxide Sheets and Polycations. *Chem. Mater.* **1999**, *11*, 771–778.
29. Luo, J. Y.; Cote, L. J.; Tung, V. C.; Tan, A. T. L.; Goins, P. E.; Wu, J. S.; Huang, J. X. Graphene Oxide Nanocolloids. *J. Am. Chem. Soc.* **2010**, *132*, 17667–17669.
30. Hong, T. K.; Lee, D. W.; Choi, H. J.; Shin, H. S.; Kim, B. S. Transparent, Flexible Conducting Hybrid Multi layer Thin Films of Multiwalled Carbon Nanotubes with Graphene Nanosheets. *ACS Nano* **2010**, *4*, 3861–3868.
31. Becerril, H. A.; Mao, J.; Liu, Z.; Stoltenberg, R. M.; Bao, Z.; Chen, Y. Evaluation of Solution-Processed Reduced Graphene Oxide Films as Transparent Conductors. *ACS Nano* **2008**, *2*, 463–470.
32. Park, S.; An, J.; Potts, J. R.; Velamakanni, A.; Murali, S.; Ruoff, R. S. Hydrazine-Reduction of Graphite- and Graphene Oxide. *Carbon* **2011**, *49*, 3019–3023.
33. Gao, X. F.; Jang, J.; Nagase, S. Hydrazine and Thermal Reduction of Graphene Oxide: Reaction Mechanisms, Product Structures, and Reaction Design. *J. Phys. Chem. C* **2010**, *114*, 832–842.
34. Stankovich, S.; Dikin, D. A.; Piner, R. D.; Kohlhaas, K. A.; Kleinhammes, A.; Jia, Y.; Wu, Y.; Nguyen, S. T.; Ruoff, R. S. Synthesis of Graphene-Based Nanosheets via Chemical Reduction of Exfoliated Graphite Oxide. *Carbon* **2007**, *45*, 1558–1565.
35. Das, A.; Pisana, S.; Chakraborty, B.; Piscanec, S.; Saha, S. K.; Waghmare, U. V.; Novoselov, K. S.; Krishnamurthy, H. R.; Geim, A. K.; Ferrari, A. C.; *et al.* Monitoring Dopants by Raman Scattering in an Electrochemically Top-Gated Graphene Transistor. *Nat. Nanotechnol.* **2008**, *3*, 210–215.
36. Ramanathan, T.; Fisher, F. T.; Ruoff, R. S.; Brinson, L. C. Amino-Functionalized Carbon Nanotubes for Binding to Polymers and Biological Systems. *Chem. Mater.* **2005**, *17*, 1290–1295.
37. Zhang, C. H.; Fu, L.; Liu, N.; Liu, M. H.; Wang, Y. Y.; Liu, Z. F. Synthesis of Nitrogen-Doped Graphene Using Embedded Carbon and Nitrogen Sources. *Adv. Mater.* **2011**, *23*, 1020–1024.
38. Sheng, Z. H.; Shao, L.; Chen, J. J.; Bao, W. J.; Wang, F. B.; Xia, X. H. Catalyst-Free Synthesis of Nitrogen-Doped Graphene via Thermal Annealing Graphite Oxide with Melamine and Its Excellent Electrocatalysis. *ACS Nano* **2011**, *5*, 4350–4358.
39. Shin, H. J.; Kim, S. M.; Yoon, S. M.; Benayad, A.; Kim, K. K.; Kim, S. J.; Park, H. K.; Choi, J. Y.; Lee, Y. H. Tailoring Electronic Structures of Carbon Nanotubes by Solvent with Electron-Donating and -Withdrawing Groups. *J. Am. Chem. Soc.* **2008**, *130*, 2062–2066.
40. Voggu, R.; Rout, C. S.; Franklin, A. D.; Fisher, T. S.; Rao, C. N. R. Extraordinary Sensitivity of the Electronic Structure and Properties of Single-Walled Carbon Nanotubes to Molecular Charge-Transfer. *J. Phys. Chem. C* **2008**, *112*, 13053–13056.
41. Guo, B. D.; Liu, Q. A.; Chen, E. D.; Zhu, H. W.; Fang, L. A.; Gong, J. R. Controllable N-Doping of Graphene. *Nano Lett.* **2010**, *10*, 4975–4980.
42. Lin, Y. C.; Lin, C. Y.; Chiu, P. W. Controllable Graphene N-Doping with Ammonia Plasma. *Appl. Phys. Lett.* **2010**, *96*, 133110.
43. Eda, G.; Chhowalla, M. Graphene-Based Composite Thin Films for Electronics. *Nano Lett.* **2009**, *9*, 814–818.
44. Kaiser, A. B.; Gomez-Navarro, C.; Sundaram, R. S.; Burghard, M.; Kern, K. Electrical Conduction Mechanism in Chemically

Derived Graphene Monolayers. *Nano Lett.* **2009**, *9*, 1787–1792.
45. Miyazaki, H.; Tsukagoshi, K.; Kanda, A.; Otani, M.; Okada, S. Influence of Disorder on Conductance in Bilayer Graphene under Perpendicular Electric Field. *Nano Lett.* **2010**, *10*, 3888–3892.
46. Hong, J.; Char, K.; Kim, B. S. Hollow Capsules of Reduced Graphene Oxide Nanosheets Assembled on a Sacrificial Colloidal Particle. *J. Phys. Chem. Lett.* **2010**, *1*, 3442–3445.
47. Kim, B. S.; Lee, S. W.; Yoon, H.; Strano, M. S.; Shao-Horn, Y.; Hammond, P. T. Pattern Transfer Printing of Multiwalled Carbon Nanotube Multilayers and Application in Biosensors. *Chem. Mater.* **2010**, *22*, 4791–4797.
48. Lee, S. W.; Kim, B. S.; Chen, S.; Shao-Horn, Y.; Hammond, P. T. Layer-by-Layer Assembly of All Carbon Nanotube Ultrathin Films for Electrochemical Applications. *J. Am. Chem. Soc.* **2009**, *131*, 671–679.
49. Lee, S. W.; Yabuuchi, N.; Gallant, B. M.; Chen, S.; Kim, B. S.; Hammond, P. T.; Shao-Horn, Y. High-Power Lithium Batteries from Functionalized Carbon-Nanotube Electrodes. *Nat. Nanotechnol.* **2010**, *5*, 531–537.
50. Zhu, J.; Shim, B. S.; Di Prima, M.; Kotov, N. A. Transparent Conductors from Carbon Nanotubes LBL-Assembled with Polymer Dopant with pi-pi Electron Transfer. *J. Am. Chem. Soc.* **2011**, *133*, 7450–7460.
51. Li, H. L.; Pang, S. P.; Wu, S.; Feng, X. L.; Mullen, K.; Bubeck, C. Layer-by-Layer Assembly and UV Photoreduction of Graphene-Polyoxometalate Composite Films for Electronics. *J. Am. Chem. Soc.* **2011**, *133*, 9423–9429.
52. Gomez-Navarro, C.; Weitz, R. T.; Bittner, A. M.; Scolari, M.; Mews, A.; Burghard, M.; Kern, K. Electronic Transport Properties of Individual Chemically Reduced Graphene Oxide Sheets. *Nano Lett.* **2007**, *7*, 3499–3503.
53. Eda, G.; Mattevi, C.; Yamaguchi, H.; Kim, H.; Chhowalla, M. Insulator to Semimetal Transition in Graphene Oxide. *J. Phys. Chem. C* **2009**, *113*, 15768–15771.